doi:10.1016/j.jmb.2009.08.016 J. Mol. Biol. (2009) 393, 227–236

JMB

Available online at www.sciencedirect.com

ScienceDirect

ELSEVIER

Effect of Macromolecular Crowding on Protein Folding Dynamics at the Secondary Structure Level

Smita Mukherjee†, Matthias M. Waegele†, Pramit Chowdhury, Lin Guo and Feng Gai*

Department of Chemistry, University of Pennsylvania, 231 South 34th Street, Philadelphia, PA 19104, USA

Received 18 June 2009; received in revised form 22 July 2009; accepted 7 August 2009
Available online 13 August 2009

Macromolecular crowding is one of the key characteristics of the cellular environment and is therefore intimately coupled to the process of protein folding *in vivo*. While previous studies have provided invaluable insight into the effect of crowding on the stability and folding rate of protein tertiary structures, very little is known about how crowding affects protein folding dynamics at the secondary structure level. In this study, we examined the thermal stability and folding–unfolding kinetics of three small folding motifs (i.e., a 34-residue α-helix, a 34-residue cross-linked helix–turn–helix, and a 16-residue β-hairpin) in the presence of two commonly used crowding agents, Dextran 70 (200 g/L) and Ficoll 70 (200 g/L). We found that these polymers do not induce any appreciable changes in the folding kinetics of the two helical peptides, which is somewhat surprising as the helix-coil transition kinetics have been shown to depend on viscosity. Also to our surprise and in contrast to what has been observed for larger proteins, we found that crowding leads to an appreciable decrease in the folding rate of the shortest β-hairpin peptide, indicating that besides the excluded volume effect, other factors also need to be considered when evaluating the net effect of crowding on protein folding kinetics. A model considering both the static and the dynamic effects arising from the presence of the crowding agent is proposed to rationalize these results.

Keywords: macromolecular crowding; confinement; protein folding; helix-coil transition; β-hairpin folding

Edited by C. R. Matthews

Introduction

Understanding how proteins fold *in vivo* poses a formidable challenge. Thus, a majority of protein folding studies have been carried out *in vitro* and under conditions wherein only dilute aqueous solutions were used. While such studies have provided invaluable insights into our understanding of the protein folding problem, these did not take into account the possible effects arising from macromolecular crowding—an important but often neglected aspect of the intracellular environment.[1–4] For instance, the presence of macromolecules near a protein could alter its folding energy landscape simply through the excluded volume effect since folding results in a compaction of the polypeptide chain.[5] Indeed, several recent experimental and computational studies have shown that such effects of volume exclusion can significantly alter the stability and folding rate of a protein.[6–16]

Besides such entropic effects, macromolecular crowding could also affect the dynamics of protein folding through other mechanisms. [In the present case, the effect of macromolecular crowding is referred to as the net effect of an inert macromolecule on the folding properties of the protein or peptide molecule in question, which includes both static effects, such as that arising from confinement, and dynamic effects, such as modulation of the frictional drag experienced by conformational motions along

*Corresponding author. E-mail address: gai@sas.upenn.edu.

† S.M. and M.M.W. contributed equally to this work.

Abbreviations used: FCS, fluorescence correlation spectroscopy; HSA, human serum albumin; HTH, helix–turn–helix; NR, Nile red; pHLIP, pH (low) insertion peptide; R6G, rhodamine 6G; T-jump, temperature jump.

the reaction coordinate.] For example, it is well known that a high-mass macromolecular crowding agent (i.e., inert polymers) not only changes the dynamic viscosity of the solution (i.e., macroviscosity) but also could modulate the microviscosity of the protein environment in which the folding reaction occurs,[17–20] thus perturbing the underlying chain dynamics, as shown by Neuweiler *et al.*[21] However, most of the experimental studies on the effects of macromolecular crowding on protein folding carried out thus far have dealt with proteins of fairly large size,[3,4,6,7,10,12–15] wherein the excluded volume effect appears to dominate, thus obscuring other subtle but important effects arising from the presence of crowding agents. In this work, we studied the folding thermodynamics and kinetics of three relatively small protein motifs in the presence of two commonly used crowding agents, Dextran 70 and Ficoll 70, with the aim of providing new insights into the effect of macromolecular crowding on folding events taking place over a relatively short length scale. These peptides form different types of protein secondary and/or supersecondary structures in solution, specifically, a 34-residue monomeric α-helix (L9:41–74),[22] a 34-residue cross-linked helix–turn–helix (HTH) motif (Z34C-m1, which is the D20A mutant of Z34C),[23] and a 16-residue β-hairpin (trpzip4-m1).[24] Given the critical importance of protein secondary structure formation in several protein folding models, such as the framework model,[25] this study is expected to also have considerable implications for the applicability of those models in describing *in vivo* protein folding.

Dextran 70 is a flexible and linear (<5% branching) polymer of D-glucopyranose that behaves as a quasi-random coil (R_h of ~63 Å),[20,26–29] whereas Ficoll 70 is a compact and highly cross-linked and branched copolymer of sucrose and epichlorohydrin that can be approximated as a semi-rigid sphere (R_h of ~55 Å).[27–29] Thus, comparative studies employing these two polymers allow one to examine how the nature and the geometric shape of the respective crowding agent affect the folding dynamics of the protein system in question. Interestingly, only the thermodynamic stability of the shortest peptide studied here (i.e., trpzip4-m1) shows an appreciable change when its environment is crowded by Ficoll 70. Similar to that observed for large proteins, macromolecular crowding leads to an increase in the thermal stability of trpzip4-m1 in the presence of 200 g/L of Ficoll 70, a concentration that falls within the concentration range that has been used in previous crowding studies.[1,2,6,7,10,11,13] However, in contrast to the common notion that macromolecular crowding increases the rate of protein folding, our results show that the folding rate of trpzip4-m1 in fact decreases in the presence of either Ficoll 70 or Dextran 70. Taken together, these results indicate that besides the commonly encountered excluded volume effect, other factors need to be considered when assessing the effect of macromolecular crowding on protein folding.

Results

All crowding experiments were carried out in 20 mM phosphate buffer in D_2O at pH 7 in the presence of either 200 g/L of Dextran 70 or 200 g/L of Ficoll 70, whereas all other experiments were carried out in 20 mM phosphate buffer in D_2O at pH 7.

L9:41–74

The far-UV circular dichroism (CD) spectra of L9:41–74 in both Dextran 70 and Ficoll 70 solutions at 4 °C exhibit the characteristic double minima of α-helices at 208 and 222 nm, respectively, and overlap with the CD spectrum of L9:41–74 in D_2O buffer solution (Figure S1). In addition, as shown in Fig. 1a, the presence of these crowding agents has little effect on the CD thermal denaturation profile of L9:41–74, indicating that the thermodynamics of the

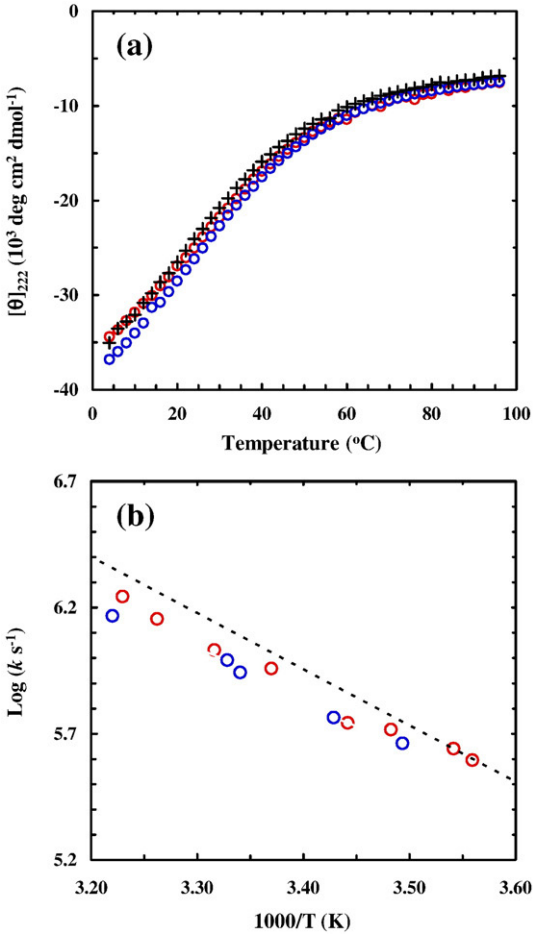

Fig. 1. (a) CD thermal melting curves of L9:41–74 in 200 g/L of Dextran 70 (red) and in 200 g/L of Ficoll 70 (blue). (b) Arrhenius plot of the T-jump-induced conformational relaxation rates of L9:41–74 in 200 g/L of Dextran 70 (red) and in 200 g/L of Ficoll 70 (blue). Also shown for comparison are the CD thermal melting curve [black crosses in (a)] and relaxation rates [black dashed line in (b)] of the same peptide in 20 mM phosphate D_2O buffer (derived from Mukherjee *et al.*[22]).

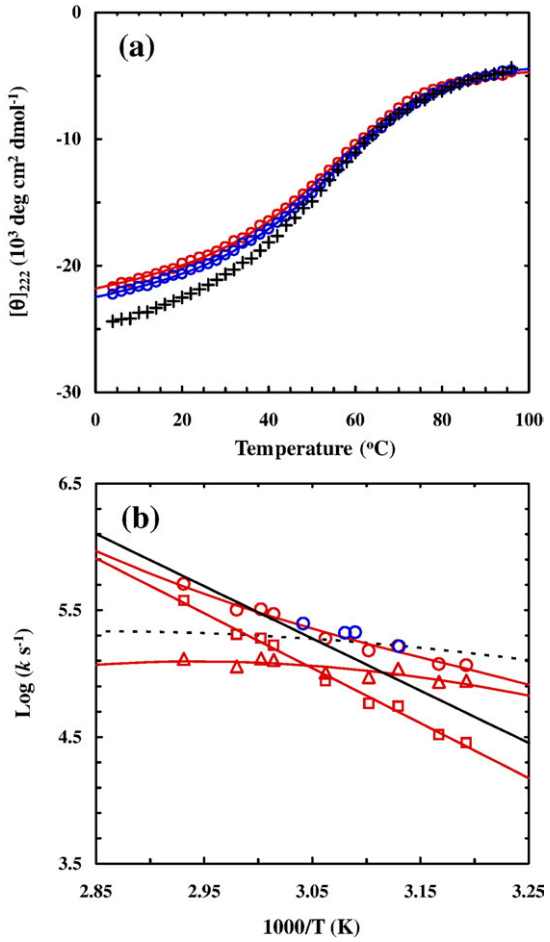

Fig. 2. (a) CD thermal melting curves of Z34C-m1 in 200 g/L of Dextran 70 (red) and in 200 g/L of Ficoll 70 (blue). Lines are global fits of these data to the two-state model described in the text. (b) Arrhenius plot of the T-jump-induced conformational relaxation rates (open circles) of Z34C-m1 in 200 g/L of Dextran 70 (red) and in 200 g/L of Ficoll 70 (blue). Open triangles and squares correspond to the two-state folding and unfolding rates of Z34C-m1 in 200 g/L of Dextran 70, respectively. Also shown are the CD thermal melting curve [black crosses in (a)] and folding [black dashed line in (b)] and unfolding [black continuous line in (b)] rate constants of Z34C-m1 in 20 mM phosphate D_2O buffer (derived from Du and Gai[23]).

underlying helix-coil transition is not sensitive to the environmental changes induced by these crowding agents.

The relaxation kinetics of L9:41–74 in these polymer solutions were studied by the laser-induced temperature jump (T-jump) infrared method, the details of which have been described elsewhere.[30] Similar to those observed in dilute solution,[22] the T-jump-induced relaxation kinetics of L9:41–74 contain two distinct phases (Figure S2). The fast phase cannot be resolved by our setup and has been attributed to temperature-induced spectral shift of the amide-I′ band.[31] On the other hand, the slow phase, which arises from the conformational redistribution process of the peptide in response to the T-jump, is well resolved and can be described by a single-exponential function. As shown in Fig. 1b, within the temperature range studied, the T-jump-induced conformational relaxation rates of L9:41–74 in both Dextran 70 and Ficoll 70 solutions are almost identical with the relaxation rate of the peptide in D_2O buffer solution. For example, at 20 °C, the relaxation time constants of L9:41–74 in Dextran 70 and Ficoll 70 solutions are 1.4±0.2 and 1.5±0.2 μs, respectively, whereas the relaxation time constant in D_2O buffer solution is 1.17±0.15 μs.[22] Taken together, these thermodynamic and kinetic results indicate that the folding–unfolding transition of this α-helical peptide is not sensitive to macromolecular crowding, at least not to that induced by 200 g/L of Dextran 70 or Ficoll 70.

Z34C-m1

The far-UV CD spectra of Z34C-m1 obtained at 4 °C in both Dextran 70 and Ficoll 70 solutions are almost completely superimposable with the CD spectrum obtained in D_2O buffer solution (Figure S3), indicating that the helical nature of the folded conformation is not affected by the crowding agents. The thermal denaturation of Z34C-m1 in both Dextran 70 and Ficoll 70 solutions, measured by monitoring the change in its helical CD signal at 222 nm with increasing temperature (Fig. 2a), also shows that these crowding agents do not change the thermal stability of the peptide to any appreciable extent. Indeed, globally fitting the CD data to a two-state model reveals that the thermal melting temperature (T_m) of Z34C-m1 in these crowded environments is only 2–3 °C higher than that[23] in D_2O buffer (Table 1). Consistent with these thermodynamic assessments, the T-jump-induced relaxation rates of Z34C-m1 in these polymer solutions also

Table 1. Summary of the thermodynamic and kinetic data for Z34C-m1 and trpzip4-m1 obtained under different conditions

	Z34C-m1			trpzip4-m1		
	D_2O buffer	Dextran 70	Ficoll 70	D_2O buffer	Dextran 70	Ficoll 70
ΔH_m (kcal mol^{-1})	16.2±0.7	17.1±0.8	16.8±0.7	13.8±0.2	12.5±0.3	15.6±0.2
ΔS_m (cal K^{-1} mol^{-1})	49.4±3.8	52.0±2.6	50.9±2.0	45.1±2.5	40.6±0.9	49.1±0.7
ΔC_p (cal K^{-1} mol^{-1})	118±34	245±105	120±54	343±41	238±19	223±15
T_m (°C)	54.7±1.0	55.3±1.5	57.7±0.5	32.1±0.9	34.3±0.5	44.0±0.2
τ_f (μs)[a]	5.3±0.8	8.6±1.3	7.3±1.1	47.5±2.3	96±14	122±18
τ_u (μs)[a]	5.1±0.8	8.8±1.3	9.0±1.4	38.1±2.0	92±14	240±36

[a] The folding and unfolding times were obtained at 55 °C for Z34C-m1 and at 35 °C for trpzip4-m1.

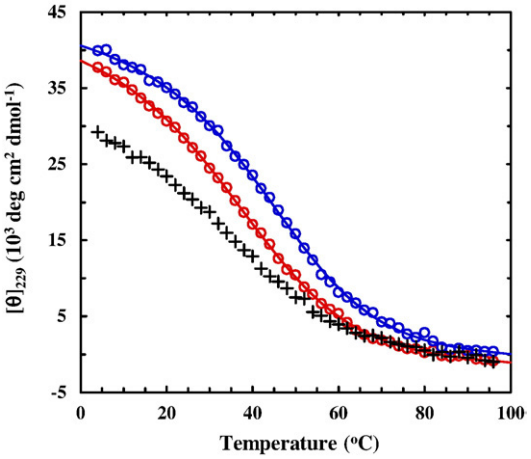

Fig. 3. CD thermal melting curves of trpzip4-m1 in 200 g/L of Dextran 70 (red) and in 200 g/L of Ficoll 70 (blue). Lines are global fits of these data to the two-state model described in the text. Also shown is the CD thermal melting curve (black) of the same peptide in 20 mM phosphate D_2O buffer (derived from Du *et al.*[24]).

show only a moderate decrease from those measured in dilute aqueous solution (Fig. 2b and Table 1).

trpzip4-m1

Similar to the CD spectrum obtained in D_2O buffer solution,[24] the far-UV CD spectra of trpzip4-m1 in both Dextran 70 and Ficoll 70 solutions exhibit a positive band centered at ~229 nm (Figure S4), arising from excitonic coupling between the paired tryptophan side chains. As shown in Fig. 3, the thermal unfolding transitions of trpzip4-m1 in these solutions, as monitored by the change in the CD signal at 229 nm, show characteristics of a cooperative thermal unfolding process. As indicated in Table 1, the thermal melting temperature (T_m) of trpzip4-m1 in Dextran 70 solution is increased only slightly compared with that (32 °C) in D_2O buffer, whereas in Ficoll 70 solution, the T_m of this peptide shows a substantial increase to ~44 °C (Table 1).

The relaxation kinetics of trpzip4-m1 in response to a T-jump were also probed at 1631 cm^{-1}, where antiparallel β-sheets are known to absorb (Figure S5).[24] As shown in Fig. 4a and b, unlike L9:41–74, the folding and unfolding rates of trpzip4-m1 are distinctly slower in the presence of the crowding agents. For example, at 35 °C, the folding and unfolding time constants of trpzip4-m1 in Dextran 70 solution are 96±14 and 92±14 μs, respectively, whereas in dilute aqueous solution,[24] this peptide folds in 47.5±2.3 μs and unfolds in 38.1±2.0 μs (Table 1).

Discussion

Since macromolecular crowding is an intrinsic feature of the cellular environment,[32,33] there has been considerable interest in recent years in investigating its effect on protein folding, both experimentally[3,4,6,7,10,12–15] and computationally.[3,4,8,9,11,13,16] However, almost all of the previous experimental efforts in this area have been focused on large proteins,[3,4,6,7,10,13–15] thus providing little, if any, information on the effect of macromolecular crowding on protein folding at the secondary structure level. While such a bias in focus is understandable because most protein secondary structural elements (e.g., monomeric α-helix and β-hairpin) are probably too small to be profoundly affected by the excluded volume effect,[3,5] understanding the influence of crowding on the folding dynamics of such small structural moieties could provide new insights into the otherwise complex interplay between different crowding effects. In addition, in view of the important role of secondary structure formation in existing protein folding models, such as the framework model,[25] there is a strong need for investigation of folding dynamics of secondary structural elements in crowded environments in

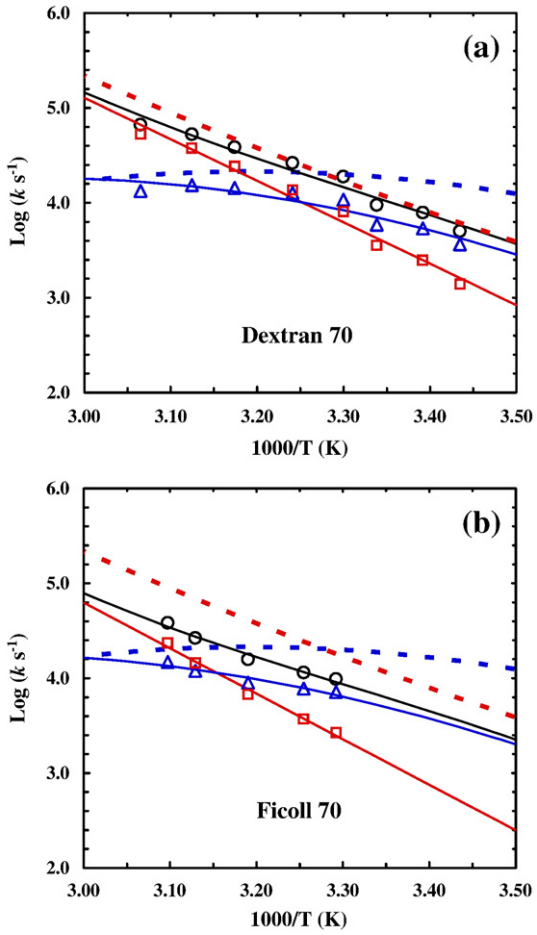

Fig. 4. Arrhenius plots of the T-jump-induced conformational relaxation rates (open circles) of trpzip4-m1 in 200 g/L of Dextran 70 (a) and in 200 g/L of Ficoll 70 (b). Open triangles and squares correspond to their respective two-state folding and unfolding rates. Also shown in each case are the folding (blue dashed line) and unfolding (red dashed line) rate constants of trpzip4-m1 in 20 mM phosphate D_2O buffer (derived from Du *et al.*[24]).

Table 2. Translational diffusion times determined by FCS at room temperature for R6G, the pHLIP peptide, and the HSA–NR complex

	D_2O	Dextran 70 (200 g/L)	Ficoll 70 (200 g/L)
R6G (μs)	53±2	216±5	256±5
pHLIP (μs)	75±3	286±5	305±8
HSA–NR (μs)	419±15	2000±30	2460±60

order to understand protein folding *in vivo*. In this work, we studied the folding thermodynamics and kinetics of three distinct secondary structural elements [i.e., a monomeric α-helix (L9:41–74), a β-hairpin (trpzip4-m1), and an HTH motif (Z34C-m1)] in the presence of two commonly used crowding agents, namely, Dextran 70 and Ficoll 70.

L9:41–74

L9:41–74 is the central α-helix of ribosomal protein L9 from the bacterium *Bacillus stearothermophilus*. Owing to a series of favorable side chain–side chain interactions, mostly electrostatic in nature, this peptide remains folded even in isolation in aqueous solution.[34] Previously, we have shown that this peptide folds on a timescale that is significantly slower than that of alanine-based peptides and that its folding time may be a more realistic representation of the timescale in which α-helices in proteins fold.[22] Thus, it would be quite interesting to further examine how crowding affects its folding–unfolding dynamics. Our CD measurements (Fig. 1a) show that the thermal stability of L9:41–74 in either Dextran 70 or Ficoll 70 solution remains practically unchanged from that in dilute aqueous solution, suggesting that the helix-coil transition experiences little, if any, crowding effect. This observation is however unexpected because the chain length of this α-helix is estimated to be 50 Å (assuming a full helical structure), which is comparable with the hydrodynamic radii of Dextran 70 and Ficoll 70.

Besides the apparent excluded volume effect, addition of a polymer to aqueous solution is also known to affect the dynamic viscosity of the solution. For example, the dynamic viscosities of 200 g/L of Dextran 70 and 200 g/L of Ficoll 70 are about 18 and 10 times greater than the dynamic viscosity of water at 20 °C,[27,35] respectively. Previously, Jas *et al*.[36] showed that the T-jump-induced relaxation rate of an alanine-based helical peptide is inversely proportional to $\eta^{0.6}$ (where η represents the viscosity of the solution) when small viscogens, such as glucose and sucrose, were used to increase the viscosity of the solution. Thus, our observation that the T-jump-induced relaxation kinetics of L9:41–74 in both Dextran 70 and Ficoll 70 solutions are almost the same as those obtained in dilute D_2O solution (Fig. 1b) is quite interesting and warrants further discussion.

The viscosity dependence of protein folding rates stems from the diffusive nature of the associated barrier-crossing events,[37–40] namely, from the requirement of polypeptide chain motion to form the stabilizing native contacts via diffusion. Previous studies have shown that under the current crowding conditions the polymer molecules can form porous networks[17,19,21] wherein the viscosity determined via the diffusion of a probe molecule can be significantly lower than the dynamic viscosity of the bulk solution.[17,21,41] To differentiate these viscosities, we referred to the one measured via molecular diffusion as the microviscosity of the solution. Since the sizes of the three peptides used in this study are relatively small, it is reasonable to assume that their folding rates would respond more to the microviscosity rather than to the dynamic viscosity of the polymer solution. Thus, to further probe the microviscosity of the current crowding solutions, we have also measured the characteristic translational diffusion times (τ_D, a quantity that is inversely proportional to the diffusion constant D) of three molecular systems of varying sizes using fluorescence correlation spectroscopy (FCS), namely, (i) a fluorescent dye [rhodamine 6G (R6G)], (ii) a 37-residue fluorescently labeled pH (low) insertion peptide (pHLIP), and (iii) the human serum albumin (HSA) protein complexed with the dye Nile red (NR). As shown in Table 2, the translational diffusion times of all three probes indicate that the microviscosities of Ficoll 70 and Dextran 70 solutions are about four to six times larger than the microviscosity of water, depending on the size of the probe and on the crowding agent.

These FCS measurements indicate that not only the dynamic (or bulk) viscosity but also the microviscosity measurements fall short of providing a rationale behind the observation that the relaxation rate of L9:41–74 is insensitive to the presence of crowding agents—this being in stark contrast to the well-documented notion that the rate of α-helix formation is susceptible to viscosity.[36,42] However, this apparent discrepancy may be reconciled by taking into account the notion that the diffusion constant could also be distance dependent.[43,44] For example, the diffusion constant (D) of a probe molecule in a polymer solution (Figure S6) consisting of porous networks[45] is:

$$D = D_0 \exp(-ac^{1/2}), \quad (1)$$

where c is the concentration of the polymer and D_0 is the diffusion constant of the probe at $c=0$. The constant a has been shown to characterize the length scale (ξ) of the pores embedded in the porous networks, at least for a simple pore model.[44] Thus, for short diffusion modes or diffusion events during which the diffusing particles travel a distance smaller than the pore size ξ of the polymer solution, the particles rarely come into contact with the polymer chains and their diffusion constant is hence close to that found in bulk water. On the other hand, for long diffusion modes or diffusion events during which the particles travel a distance much larger than ξ, the resultant diffusion constant

becomes smaller than that measured in bulk water, similar to the diffusion constants observed in our FCS measurements. In this context, it is clear that the viscosity effect exerted by a polymeric crowding agent on the folding rate of a peptide depends on the length scale that the polypeptide chain has to traverse from the unfolded state to the transition state along the folding coordinate.

The formation of an α-helix can be regarded as a series of local events wherein a hydrogen bond between the amino acids at "*i*" and "*i*+4" positions along the polypeptide chain is formed. Thus, the length scale (a few angstrom) over which the key α-helix folding events take place is far less than the pore size of the polymer solutions used in the current study and the corresponding folding rate therefore does not show any significant deviation from that in dilute aqueous solution. In contrast, in studies where small viscogens (e.g., glucose and sucrose) are used to increase the viscosity, the resulting solution viscosity is microscopically homogeneous and the effect of increased solvent friction can therefore be experienced down to a very short length scale. Thus, in such cases, the viscosity dependence of the folding kinetics of protein secondary structural elements might become more pronounced, as has been shown in a previous study.[36]

Z34C-m1

Z34C-m1 is a mutant of Z34C (i.e., D20A) that forms a crossed-linked HTH structure, a common structural motif found in DNA-binding proteins.[46] We have previously shown that Z34C-m1 folds significantly slower than Z34C does since the mutation deletes a hydrogen bond that is critical to the stability of the reverse turn.[23] Z34C-m1 constitutes a good model system to further examine the effect of microviscosity on the folding–unfolding kinetics of α-helices in a protein context as the disulfide cross-linker prevents the protein to become extended upon unfolding and hence makes it less likely to experience the excluded volume effect. As expected, the folding thermodynamics and kinetics of Z34C-m1 are only moderately affected by the crowding agents employed herein (Fig. 2a and b and Table 1). Thus, these results are consistent with those for L9:41–74 and further corroborate the notion that macromolecular crowding does not affect to any significant extent the folding dynamics of α-helices that can fold independently. However, in a protein context, the frictional drag along the folding coordinate of an α-helix may be position dependent and thus could exert a more complex effect on the folding dynamics. Apparently, for β-sheets whose folding requires relatively large-scale chain diffusions, the effect of microviscosity is expected to play a more important role, as discussed below.

trpzip4-m1

To further explore the extent to which the nature of the folded topology determines the effect of macromolecular crowding, we have also studied the folding thermodynamics and kinetics of trpzip4-m1, the D46A mutant of the 16-residue β-hairpin trpzip4[24] in both Dextran 70 and Ficoll 70 solutions. While the thermal denaturation properties of trpzip4-m1 are almost unaffected by addition of Dextran 70, its thermal melting temperature in Ficoll 70 solution shows a substantial increase from that in D_2O buffer.[24] This difference manifests the disparity in terms of crowding efficiency of these crowding agents and can be rationalized based on the overall difference in the molecular structures of these polymers. Previous studies have shown that the persistence length of Dextran is about 0.4 nm,[47] which renders it to be a relatively flexible polymer. On the other hand, Ficoll 70 is comparatively more rigid due to its cross-linked structure.[29,48] Thus, based on these considerations, it is conceivable that Dextran 70 can accommodate more interstitial spaces in comparison with Ficoll 70 at the same concentration, therefore allowing the unfolded polypeptide chain of trpzip4-m1 more space to escape and hence leading to a weaker excluded volume effect.

In contrast to that observed in other studies,[6,9,11] macromolecular crowding results in a decrease in the folding rate of trpzip4-m1. This result thus clearly indicates that a macromolecular crowding agent can affect not only the protein stability via the excluded volume effect but also the folding dynamics through modulation of the effective viscosity of the protein environment. In the case of Dextran 70, the thermal stability of the β-hairpin exhibits only a very modest change (Table 1), thus implying that the observed reduction in the folding and unfolding rates is unlikely to result from the excluded volume effect and rather arises from a viscosity effect. This interpretation is consistent with the notion that the dynamics of peptide loop closure and β-hairpin folding require relatively large-scale and nonlocal motions, in contrast to the folding of an α-helix, wherein the chain primarily undergoes a series of local structural reorganizations. Thus, during such a folding event, the peptide chain has a higher chance of colliding with the polymer network formed by the crowding molecules, resulting in a slower folding–unfolding rate. This picture is consistent with a recent FCS study by Neuweiler *et al.*,[21] who showed that the intrachain diffusion rate of a series of fluorescently labeled short poly(GS)-peptides in Ficoll 70 depends on the net effect of two opposing forces: the excluded volume effect and the increased viscous drag of the polymer solution.

The effect of viscosity on protein folding or unfolding rate constant (k_{obs}) can often be described by the hydrodynamic approximation of the Kramers equation in the high friction limit; that is,

$$k_{obs} = \frac{A}{\eta(T)^{\alpha}} \exp(-\Delta G^{\neq}/RT), \qquad (2)$$

where $\eta(T)$ is the effective viscosity of the medium at temperature T and has been assumed here to be

independent of the spatial location of the peptide, α is equal to unity in many cases, A is a constant, $\Delta G^{\neq}$ is the apparent free-energy barrier at temperature T, and R is the gas constant. Thus, a crowding agent can modulate the folding and unfolding rate constants of a protein by changing η, $\Delta G^{\neq}$, or both. Apparently, the effect related to η is a dynamic one, whereas that related to $\Delta G^{\neq}$ is static (or the excluded volume) in nature.

For a simple two-state scenario, assuming that A is the same for both folding and unfolding and that it is independent of crowding, one can easily show that (irrespective of the position of the transition state)

$$\ln\left(\frac{k_f^c}{k_f^0}\right) + \ln\left(\frac{k_u^c}{k_u^0}\right) = 2\alpha\ln\left(\frac{\eta_0(T)}{\eta_c(T)}\right) + \frac{1}{RT}(\Delta G_u^{c-0} + \Delta G_f^{c-0}), \quad (3)$$

where k_f and k_u are the folding and unfolding rate constants, respectively; $\Delta G_u^{c-0} = G_u^c - G_u^0$ and $\Delta G_f^{c-0} = G_f^c - G_f^0$, where G_u and G_f represent the free energies of the unfolded and folded states, respectively; and, in all cases, the superscripts "0" and "c" represent the dilute and crowded solutions, respectively. In addition, $\eta_0(T)$ and $\eta_c(T)$ are the effective viscosities of the dilute and crowded solutions at temperature T, respectively. For Dextran 70, the increased stabilization of the β-hairpin conformation of trpzip4-m1 arising from crowding is considered to be negligible (i.e., $\Delta G_u^{c-0} + \Delta G_f^{c-0} \approx 0$). Thus, with the use of the measured folding and unfolding rate constants of trpzip4-m1 in the presence and in the absence of crowding agents, in conjunction with the assumption that α is approximately unity for β-hairpin folding,[36] the value of η_c/η_0 is calculated to be 3.5±0.5 at 20 °C, which is comparable with the ratio of diffusion times $\tau_c/\tau_0 = 3.8$ of the pHLIP peptide in 200 g/L of Dextran 70 and in water at room temperature (Table 2). Therefore, this agreement further corroborates the idea that Dextran 70 affects trpzip4-m1 folding via mostly the dynamic (or viscosity) effect.

In the case of Ficoll 70, the presence of the crowding agent leads to not only a decrease in the folding rate of trpzip4-m1 but also a significant increase in the stability of β-hairpin conformation (Figs. 3 and 4b and Table 1), indicating that the folding and unfolding dynamics of trpzip4-m1 experience both the excluded volume and viscosity effects. As a result, the unfolding rate is decreased to a larger extent than the folding rate, compared with their respective values in D_2O buffer solution (Table 1). This is because both the excluded volume and viscosity effects slow the rate of unfolding, whereas they exhibit opposite effects on the folding rate.

Furthermore, it is easy to show that

$$\frac{k_f^c}{k_f^0} = \left(\frac{\eta_0}{\eta_c}\right)^{\alpha} \exp\left(\frac{\Delta\Delta G^{\neq}}{RT}\right), \quad (4)$$

where $\Delta\Delta G^{\neq} = \Delta G_0^{\neq} - \Delta G_c^{\neq}$, which is a quantitative measure of the excluded volume effect on the folding dynamics. Thus, it is possible to dissect the static and dynamic contributions to the total crowding effect if η_c/η_0 is known. While η_c/η_0 cannot be determined independently from the current study, the result obtained with Dextran 70 nevertheless suggests that it approaches the τ_c/τ_0 ratio measured by the FCS method. Thus, using the ratio $\tau_c/\tau_0 = 4.1$ (Table 2), we estimated the $\Delta\Delta G^{\neq}$ value to be 0.3±0.1 kcal mol^{-1} at 35 °C for the folding of trpzip4-m1 in 200 g/L of Ficoll 70 solution. As expected, the decrease in the folding free-energy barrier of trpzip4-m1 due to the excluded volume effect is very modest, as the additional stabilization (i.e., $\Delta\Delta G^0 = |\Delta G_c^0| - |\Delta G_0^0|$) of trpzip4-m1 due to the presence of 200 g/L of Ficoll 70 at 35 °C is only about 0.5±0.1 kcal mol^{-1}, owing to the small size of the peptide relative to the size of the crowding agent, which is in agreement with the theoretical prediction by Minton.[5] However, we expect that the approach outlined above will be very useful for dissecting the static and dynamic effects of a crowding agent for other protein systems.

Conclusions

Employing two commonly used crowding agents, Dextran 70 (200 g/L) and Ficoll 70 (200 g/L), we have studied how macromolecular crowding affects the folding–unfolding kinetics of three peptides that fold into different conformations in solution, namely, an α-helix (L9:41–74), a cross-linked HTH (Z34C-m1), and a β-hairpin (trpzip4-m1). Interestingly, only the folding thermodynamics and kinetics of the shortest peptide, trpzip4-m1, were found to show significant changes in the Ficoll 70 solution, thus indicating that the effect of macromolecular crowding is sensitive to the size and the shape of both the peptide and the crowding agent. In addition, the observation that macromolecular crowding does not significantly alter the folding dynamics of the two helical peptides is consistent with the notion that α-helix formation involves mostly local interactions. Furthermore, and in contrast to that observed for large proteins, macromolecular crowding results in a decrease in the folding rate of trpzip4-m1, indicating that the motion of the peptide chain experiences higher friction arising from the presence of the crowding agent and that the viscosity effect in this case outplays the excluded volume effect on the folding kinetics of the β-hairpin.

Materials and Methods

Peptide synthesis and purification

All peptides used in this study were synthesized based on standard Fmoc protocols on a PS3 automated peptide synthesizer (Protein Technologies, MA) and purified by reversed-phase chromatography. The peptide sequences are as follows: Ac-41PANLKALEAQ-51KQKEQRQAAE-61ELANAKKLKE-71QLEK-NH_2 (L9:

41–74), 6FNMQCQRRFY-16EALHAPNLNE-26EQRNA-KIKSI-36RDDC-NH_2 (Z34C-m1), and GEWTWADATK-TWTWTE-NH_2 (trpzip4-m1). TMR maleimide (Molecular Probes, CA), a thiol reactive dye, was used to label the cysteine variant of pHLIP peptide[49] (sequence: ACEQN-PIYWA-RYADWLFTTP-LLLLDLALLV-DADEGTG) following the protocol available in the Molecular Probes handbook. Oxidation of the Z34C mutant was done as previously described.[23] The identity of the peptide sample was further verified by matrix-assisted laser desorption ionization mass spectroscopy. Multiple rounds of lyophilization against a solution of 0.1 M DCl/D_2O were used to remove the exchangeable hydrogen atoms and the residual trifluoroacetic acid from the peptide synthesis. Peptide solutions used in both CD and infrared measurements were prepared by directly dissolving lyophilized peptide solids in 20 mM phosphate buffer, pH 7, with or without the presence of the crowding agent. The final peptide concentration for L9:41–74 was determined by comparing the published CD data,[34] and the concentrations for other peptides were determined as previously described[23,24] and were about 16–134 μM and 0.8–1.5 mM for CD and infrared samples, respectively.

Crowding agents

Dextran 70 and Ficoll 70 were purchased from Fisher Scientific (PA) and GE Healthcare (NJ), respectively, and were used as received.

CD spectroscopy

All CD data were collected on an Aviv 62A DS CD spectrometer (Aviv Associate, NJ). The folding–unfolding thermodynamics of each peptide were obtained by fitting its CD thermal melting transition obtained at either 222 nm (for the helical peptides) or 229 nm (for the β-hairpin) to a two-state model described in detail previously.[50]

Infrared T-jump setup

The time-resolved T-jump infrared apparatus used in the current study has been described in detail elsewhere.[30] The relaxation kinetics of all peptides in response to a T-jump were probed at 1631 cm^{-1}. The observed relaxation rate constants (k_R) were further separated into folding (k_f) and unfolding (k_u) rate constants based on the thermodynamic results obtained from CD studies using the following equations:

$$k_R = k_f + k_u \tag{5}$$

$$K_{eq} = k_f / k_u \tag{6}$$

Fluorescence correlation spectroscopy

Details of the FCS setup have been described elsewhere.[51] For each measurement, either 1 nM R6G or 1 nM TMR-labeled pHLIP peptide solution or a solution of 40 nM NR and 20 μM HSA was loaded on PEG (polyethylene glycol)-silane (Gelest Inc., Morrisville, PA)-modified glass slip. Excitation of the dye was accomplished by the 514-nm line of an Ar^+ ion laser (~100 μW before entering the microscope), and the resultant fluorescence was equally split by a nonpolarizing beamsplitter (Newport Corporation, CA) and detected by two avalanche photodiodes (Perkin Elmer, NJ) using an integration time of 0.1 μs. Correlating the fluorescence signals in the cross-correlation mode was accomplished by a Flex 03-LQ-01 correlator card (Correlator.com, NJ) for a duration of 120 s, and the resulting autocorrelation traces were analyzed using the following equation:[52]

$$G(\tau) = \left(\sum_{i=1}^{n} \frac{1}{N} \left(\frac{f_i}{1 + \frac{\tau}{\tau_D^i}} \right) \left(\frac{1}{1 + \frac{\tau}{\omega^2 \tau_D^i}} \right)^{1/2} \right) \times \left(1 - T + T \cdot e^{-\frac{\tau}{\tau_T}} \right), \tag{7}$$

where τ_D^i represents the characteristic diffusion time constant of species i, ω refers to the axial-to-lateral dimension ratio of the confocal volume element, N represents the number of fluorescent molecules in the confocal volume, f_i represents the fraction of species i, τ_T is the triplet lifetime of the fluorophore, and T represents the corresponding triplet amplitude.

Acknowledgement

We gratefully acknowledge financial support from the National Institutes of Health (GM-065978 and RR-01348).

Supplementary Data

Supplementary data associated with this article can be found, in the online version, at doi:10.1016/j.jmb.2009.08.016

References

1. Ellis, R. J. (2001). Macromolecular crowding: obvious but underappreciated. *Trends Biochem. Sci.* **26**, 597–604.
2. Minton, A. P. (2001). The influence of macromolecular crowding and macromolecular confinement on biochemical reactions in physiological media. *J. Mol. Biol.* **276**, 10577–10580.
3. Zhou, H.-X., Rivas, G. & Minton, A. P. (2008). Macromolecular crowding and confinement: biochemical, biophysical, and potential physiological consequences. *Annu. Rev. Biophys.* **37**, 375–397.
4. Zhou, H.-X. (2008). Protein folding in confined and crowded environments. *Arch. Biochem. Biophys.* **469**, 76–82.
5. Minton, A. P. (2005). Models for excluded volume interaction between an unfolded protein and rigid macromolecular cosolutes: macromolecular crowding and protein stability revisited. *Biophys. J.* **88**, 971–985.
6. van den Berg, B., Wain, R., Dobson, C. M. & Ellis, R. J. (2000). Macromolecular crowding perturbs protein refolding kinetics: implications for folding inside the cell. *EMBO J.* **18**, 6927–6933.
7. Qu, Y. X. & Bolen, D. W. (2002). Efficacy of macromolecular crowding in forcing proteins to fold. *Biophys. Chem.* **101**, 155–165.
8. Friedel, M., Sheeler, D. J. & Shea, J. E. (2003). Effects of confinement and crowding on the thermodynamics and kinetics of folding of a minimalist beta-barrel protein. *J. Chem. Phys.* **118**, 8106–8113.

9. Ping, G., Yuan, J. M., Sun, Z. F. & Wei, Y. (2004). Studies of effects of macromolecular crowding and confinement on protein folding and protein stability. *J. Mol. Recognit.* **17**, 433–440.
10. Tokuriki, N., Kinjo, M., Negi, S., Hoshino, M., Goto, Y., Urabe, I. & Yomo, T. (2004). Protein folding by the effects of macromolecular crowding. *Protein Sci.* **13**, 113–125.
11. Cheung, M. S., Klimov, D. & Thirumalai, D. (2005). Molecular crowding enhances native state stability and refolding rates of globular proteins. *Proc. Natl Acad. Sci. USA*, **102**, 4753–4758.
12. Ai, X. J., Zhou, Z., Bai, Y. W. & Choy, W.-Y. (2006). N-15 NMR spin relaxation dispersion study of the molecular crowding effects on protein folding under native condition. *J. Am. Chem. Soc.* **128**, 3916–3917.
13. Yuan, J. M., Chyan, C.-L., Zhou, H.-X., Chung, T.-Y., Peng, H. B., Ping, G. H. & Yang, G. L. (2008). The effects of macromolecular crowding on the mechanical stability of protein molecules. *Protein Sci.* **17**, 2156–2166.
14. Charlton, L. M., Barnes, C. O., Li, C. G., Orans, J., Young, G. B. & Pielak, G. J. (2008). Residue-level interrogation of macromolecular crowding effects on protein stability. *J. Am. Chem. Soc.* **130**, 6826–6830.
15. Homouz, D., Stagg, L., Wittung-Stafshede, P. & Cheung, M. S. (2009). Macromolecular crowding modulates folding mechanism of alpha/beta protein apoflavodoxin. *Biophys. J.* **96**, 671–680.
16. Rivera, E., Straub, J. & Thirumalai, D. (2009). Sequence and crowding effects in the aggregation of a 10-residue fragment derived from islet amyloid polypeptide. *Biophys. J.* **96**, 4552–4560.
17. Lavalette, D., Tetreau, C., Tourbez, M. & Blouquit, Y. (1999). Microscopic viscosity and rotational diffusion of proteins in a macromolecular environment. *Biophys. J.* **76**, 2744–2751.
18. Kozer, N. & Schreiber, G. (2004). Effect of crowding on protein–protein association rates: fundamental differences between low and high mass crowding agents. *J. Mol. Biol.* **336**, 763–774.
19. Kozer, N., Kuttner, Y. Y., Haran, G. & Schreiber, G. (2007). Protein–protein association in polymer solutions: from dilute to semidilute to concentrated. *Biophys. J.* **92**, 2139–2149.
20. Goins, A. B., Sanabria, H. & Waxham, M. N. (2008). Macromolecular crowding and size effects on probe microviscosity. *Biophys. J.* **95**, 5362–5373.
21. Neuweiler, H., Löllmann, M., Doose, S. & Sauer, M. (2007). Dynamics of unfolded polypeptide chains in crowded environment studied by fluorescence correlation spectroscopy. *J. Mol. Biol.* **365**, 856–869.
22. Mukherjee, S., Chowdhury, P., Bunagan, M. R. & Gai, F. (2008). Folding kinetics of a naturally occurring helical peptide: implication of the folding speed limit of helical proteins. *J. Phys. Chem. B*, **112**, 9146–9150.
23. Du, D. & Gai, F. (2006). Understanding the folding mechanism of an alpha-helical hairpin. *Biochemistry*, **45**, 13131–13139.
24. Du, D., Tucker, M. J. & Gai, F. (2006). Understanding the mechanism of beta-hairpin folding via phi-value analysis. *Biochemistry*, **45**, 2668–2678.
25. Kim, P. S. & Baldwin, R. L. (1982). Specific intermediates in the folding reactions of small proteins and the mechanism of protein folding. *Annu. Rev. Biochem.* **51**, 459–489.
26. Ruhlmann, C., Thieme, M. & Helmstedt, M. (2001). Interaction between dextran and human low density lipoproteins (LDL) observed using laser light scattering. *Chem. Phys. Lipids*, **110**, 173–181.
27. Wenner, J. R. & Bloomfield, V. A. (1999). Crowding effects on EcoRV kinetics and binding. *Biophys. J.* **77**, 3234–3241.
28. Luby-Phelps, K., Castle, P. E., Taylor, D. L. & Lanni, F. (1987). Hindered diffusion of inert tracer particles in the cytoplasm of mouse 3T3 cells. *Proc. Natl. Acad. Sci. USA*, **84**, 4910–4913.
29. Venturoli, D. & Rippe, B. (2005). Ficoll and dextran vs. globular proteins as probes for testing glomerular permselectivity: effects of molecular size, shape, charge, and deformability. *Am. J. Physiol.* **288**, F605–F613.
30. Huang, C.-Y., Getahun, Z., Zhu, Y., Klemke, J. W., DeGrado, W. F. & Gai, F. (2002). Helix formation via conformation diffusion search. *Proc. Natl. Acad. Sci. USA*, **99**, 2788–2793.
31. Mukherjee, S., Chowdhury, P. & Gai, F. (2007). Infrared study of the effect of hydration on the amide I band and aggregation properties of helical peptides. *J. Phys. Chem. B*, **111**, 4596–4602.
32. Fulton, A. B. (1982). How crowded is the cytoplasm? *Cell*, **30**, 345–347.
33. Zimmerman, S. B. & Trach, S. O. (1991). Estimation of macromolecule concentrations and excluded volume effects for the cytoplasm of *Escherichia coli*. *J. Mol. Biol.* **222**, 599–620.
34. Kuhlman, B., Yang, H. Y., Boice, J. A., Fairman, R. & Raleigh, D. P. (1997). An exceptionally stable helix from the ribosomal protein L9: implications for protein folding and stability. *J. Mol. Biol.* **270**, 640–647.
35. Phillies, G. D. J. & Quinlan, C. A. (1992). Glass temperature effects on probe diffusion in dextran solutions. *Macromolecules*, **25**, 3110–3116.
36. Jas, G. S., Eaton, W. A. & Hofrichter, J. (2001). Effect of viscosity on the kinetics of alpha-helix and beta-hairpin formation. *J. Phys. Chem. B*, **105**, 261–272.
37. Jacob, M. & Schmid, F. X. (1999). Protein folding as a diffusional process. *Biochemistry*, **38**, 13773–13779.
38. Bhattacharyya, R. P. & Sosnick, T. R. (1999). Viscosity dependence of the folding kinetics of a dimeric and monomeric coiled coil. *Biochemistry*, **38**, 2601–2609.
39. Hagen, S. J., Qiu, L. L. & Pabit, S. A. (2005). Diffusional limits to the speed of protein folding: fact or friction? *J. Phys.: Condens. Matter*, **17**, S1503–S1514.
40. Frauenfelder, H., Fenimore, P. W., Chen, G. & McMahon, B. H. (2006). Protein folding is slaved to solvent motions. *Proc. Natl. Acad. Sci. USA*, **103**, 15469–15472.
41. Barshtein, G., Almagor, A., Yedgar, S. & Gavish, B. (1995). Inhomogeneity of viscous aqueous solutions. *Phys. Rev. E: Stat. Phys., Plasmas, Fluids, Relat. Interdiscip. Top.* **52**, 555–557.
42. Klimov, D. K. & Thirumalai, D. (1997). Viscosity dependence of the folding rates of proteins. *Phys. Rev. Lett.* **79**, 317–320.
43. Masuda, A., Ushida, K., Koshino, H., Yamashita, K. & Kluge, T. (2001). Novel distance dependence of diffusion constants in hyaluronan aqueous solution resulting from its characteristic nano-microstructure. *J. Am. Chem. Soc.* **123**, 11468–11471.
44. Masuda, A., Ushida, K., Nishimura, G., Kinjo, M., Tamura, M., Koshino, H. *et al.* (2004). Experimental evidence of distance-dependent diffusion coefficients of a globular protein observed in polymer aqueous solution forming a network structure on nanometer scale. *J. Chem. Phys.* **121**, 10787–10793.
45. Ogston, A. G., Preston, B. N. & Wells, J. D. (1973).

Transport of compact particles through solutions of chain-polymers. *Proc. R. Soc. London, Ser. A*, **333**, 297–316.
46. Starovasnik, M. A., Braisted, A. C. & Wells, J. A. (1997). Structural mimicry of a native protein by a minimized binding domain. *Proc. Natl. Acad. Sci. USA*, **94**, 10080–10085.
47. Rief, M., Fernandez, J. M. & Gaub, H. E. (1998). Elastically coupled two-level systems as a model for biopolymer extensibility. *Phys. Rev. Lett.* **81**, 4764–4767.
48. Bohrer, M. P., Patterson, G. D. & Carroll, P. J. (1984). Hindered diffusion of dextran and Ficoll in microporous membranes. *Macromolecules*, **17**, 1170–1173.
49. Reshetnyak, Y. K., Segala, M., Andreev, O. A. & Engelman, D. M. (2007). A monomeric membrane peptide that lives in three worlds: in solution, attached to, and inserted across lipid bilayers. *Biophys. J.* **93**, 2363–2372.
50. Bunagan, M. R., Gao, J. M., Kelly, J. W. & Gai, F. (2009). Probing the folding transition state structure of the villin headpiece subdomain via side chain and backbone mutagenesis. *J. Am. Chem. Soc.* **131**, 7470–7476.
51. Guo, L., Chowdhury, P., Fang, J. Y. & Gai, F. (2007). Heterogeneous and anomalous diffusion inside lipid tubules. *J. Phys. Chem. B*, **111**, 14244–14249.
52. Haustein, E. & Schwille, P. (2007). Fluorescence correlation spectroscopy: novel variations of an established technique. *Annu. Rev. Biophys. Biomol. Struct.* **36**, 151–169.